ACS OMEGA

http://pubs.acs.org/journal/acsodf

Article

Chemical Activation of Forage Grass-Derived Biochar for Treatment of Aqueous Antibiotic Sulfamethoxazole

Shengquan Zeng and Eunsung Kan*

Cite This: *ACS Omega* 2020, 5, 13793−13801

Read Online

ACCESS | Metrics & More | Article Recommendations | Supporting Information

ABSTRACT: Chemically activated forage Bermudagrass-derived biochar (A-BC) was produced, characterized, and utilized for adsorption of sulfamethoxazole (SMX) in water for the first time. After NaOH activation, A-BC showed a higher surface area (1991.59 m^2/g) and maximum adsorption capacity for SMX (425 mg SMX/g BC) than those of various biochars and commercial activated carbons. The detailed analysis for adsorption of SMX onto A-BC indicated the efficient sorption of SMX through $\pi-\pi$ EDA and hydrophobic and hydrogen bond interactions. Additionally, the adsorption of SMX on A-BC was limited by pore and liquid film diffusions. The SMX adsorption on A-BC was found to be endothermic and spontaneous from thermodynamic studies. Furthermore, the highly efficient regeneration of SMX-saturated A-BC over multiple cycles was achieved by NaOH-driven desorption, indicating that the adsorption of SMX onto A-BC would have high potential for cost-effective solution for elimination of SMX from water.

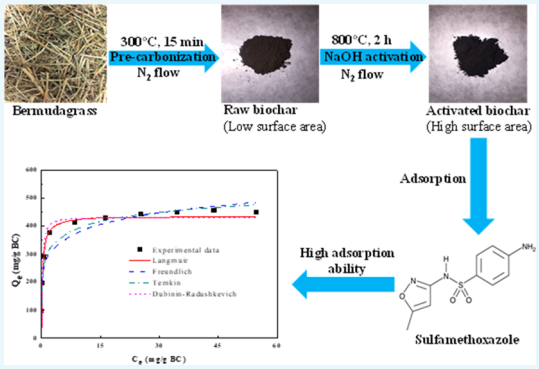

1. INTRODUCTION

Sulfamethoxazole (SMX), one of the extensively used sulfonamide antibiotics, can treat various diseases and infections in human and animals.[1] However, SMX has been detected in various water bodies and soil, causing toxic effects in aquatic organisms and prevalence of antibiotic resistance genes because of its widespread utilization, low metabolic efficiency, and slow biodegradation.[1−3] Given its environmental impacts, it is significant to effectively eliminate the antibiotic SMX from water and wastewater.

Various treatment methods including ozonation, photolysis, electrochemical oxidation, and adsorption have been applied for eliminating SMX from water.[1] Among these techniques, adsorption has been recognized as a low-cost and practically feasible process owing to its simple and effective removal of SMX and no generation of toxic intermediates and by-products.[3,4] Up to now, carbon nanotubes,[5] graphene oxide,[6] activated carbon (AC),[7] and clay mineral[8] have been investigated to remove SMX in water. However, compared to low-cost waste-derived biochars (BCs), these adsorbents are less economically feasible and environmentally sustainable because of relatively higher costs for manufacturing, regeneration, and disposal, which hinder their practical applications.

BCs, produced from pyrolysis of biomass under limited oxygen conditions, have been actively studied for their applications for removal of contaminants in water, soil, and air.[9,10] It has been reported that BCs can interact with sulfonamide antibiotics through van der Waals, $\pi-\pi$, hydrogen bonding, and electrostatic interactions.[11] A variety of BCs derived from alfalfa grass,[12] wood sawdust,[9] bagasse,[3] wheat straw, and rice straw[8] have been utilized for treatment of SMX in water. However, these raw BCs exhibited low adsorption capacities (less than 100 mg/g BC) with their less-developed pore structures and low surface areas (Table S1).[1,4]

Activation has been recognized as an effective method to improve the surface area and enhance the pore volume of BCs.[10] Activation of BCs has been studied via physical (e.g., steam and CO_2), chemical (e.g., NaOH, KOH, and H_3PO_4), and catalytic methods.[4,10,13−16] However, studies for SMX adsorption onto the activated BCs have been rarely reported. The H_3PO_4 activation of bamboo resulted in improvement of the surface area and pore volume of BC from 0.5 m^2/g and 0.00053 cm^3/g to 1.12 m^2/g and 0.0023 cm^3/g, respectively, while enhancing the adsorption capacity of this activated BC for SMX up to 88.10 mg SMX/g BC.[13] Moreover, the effective adsorption of SMX (397.29 mg/g BC) using the NaOH-activated *Pinus taeda* BC was achieved by the high surface area (959.9 m^2/g) and hydrophobicity.[1]

In addition, the source and availability of feedstock are very important for production of BC in terms of production cost and environmental sustainability. Bermudagrass (BG), as one of the most abundant forage grasses in USA, is widely grown in

Received: March 4, 2020
Accepted: May 22, 2020
Published: June 3, 2020

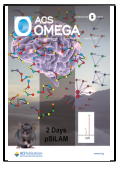

Table 1. Physicochemical Characteristics of all BCs[a]

	elemental analysis (wt %)							
	C	H	O	N	S	H/C	O/C	(N + O)/C
BG	47.43	6.30	35.66	2.5	0.42	1.60	0.56	0.61
R-BC	59.53	5.07	27.56	4.20	0.09	1.02	0.35	0.41
BC800	68.02	1.58	12.94	3.37	0.05	0.28	0.14	0.19
A-BC	81.22	0.84	7.42	0.83	0.23	0.12	0.07	0.08
	proximate analysis (%, dry basis)							
	FC	VC	ash	BET Surface area (m^2/g)		yield (%)	pH_{PZC}	
BG	6.60	85.71	7.69	0.63				
R-BC	23.22	73.14	3.64	1.67		62.05	5.07	
BC800	67.92	18.04	14.04	85.82		29.27	4.19	
A-BC	70.96	19.58	9.46	1991.59		8.91	5.63	

[a]BG: Bermudagrass; R-BC: raw biochar produced at 300 °C; BC800: biochar produced at 800 °C; A-BC: activated biochar; FC: fixed carbon; VC: volatile carbon.

the southeast part of USA with an annual dry matter yield of 6−10 tons per acre.[17] Moreover, about 20% of these forage grasses are often discarded because of generation of pathogenic fungi in the forage grasses under excessive moisture conditions during their storage at farms, while the fungi-infected forages can cause severe diseases in animals.[18] Considering high quantities of BG production including discarded ones, BG could be potentially a viable biomass feedstock for BC production. However, the preparation and application of BG-derived BCs have been rarely studied, except that the previous studies mentioned that BG-derived BC could be applied for the treatment of tetracycline and chromium in water.[18,19]

Although $ZnCl_2$, NaOH, KOH, H_3PO_4, and $FeCl_3$ are commonly used as chemical and catalytic activating agents, zinc cations are toxic in aqueous solution, while phosphoric acid is very hazardous and can cause damage to the skin, eyes, mouth, and respiratory tract. In addition, compared to KOH, NaOH is more environmentally friendly and less corrosive.[4] In our preliminary study, NaOH and $FeCl_3$ as the activating agents were used to make activated BG-derived BCs under the same pyrolysis conditions. The results showed that the NaOH-activated BG BC had a larger surface area (1992 m^2/g) and higher SMX adsorption capacity (425 mg SMX/g BC) than those of $FeCl_3$-activated BG BC (1013 m^2/g and 253 mg/g BC) under the same adsorption conditions (100 mL of 100 mg/L SMX, initial pH of 3, 0.01 g BC, and 3 d). Hence, in this study, the NaOH-activated BG BC was used for the detailed characterization and adsorption experiments.

For the first time, this work studied the detailed characteristics and mechanism about SMX adsorption on the NaOH-activated forage BG BC (A-BC) through isotherm, kinetic, and thermodynamic studies. Therefore, the major objectives of this research were the production and characterization of A-BC and its application for SMX adsorption from water. The batch experiments for the isotherm, kinetic, and thermodynamic studies were conducted, while highly efficient NaOH-driven regeneration of SMX-saturated A-BC was developed. Based on the detailed investigation of physicochemical properties and adsorption characteristics, possible mechanisms associated with adsorption of SMX onto A-BC were also elucidated.

2. RESULTS AND DISCUSSION

2.1. Characterization of BCs. The physicochemical properties of all BCs produced in this study are listed in Table 1. The A-BC showed a significantly increased Brunauer−Emmett−Teller (BET) surface area of 1991.59 m^2/g compared with R-BC (raw biochar produced at 300 °C, 1.67 m^2/g) and BC800 (biochar produced at 800 °C, 85.82 m^2/g). During NaOH activation at high temperature, the stoichiometric reaction between NaOH and carbon can be described as the following equation[4]

$$6NaOH + 2C \rightarrow 2Na + 2Na_2CO_3 + 3H_2\uparrow \quad (1)$$

Thus, the high surface area of A-BC can result from pore enlargement, which is associated with the following pathways: (1) evolution of carbon monoxide, carbon dioxide, and hydrogen produced from the breakdown of Na_2CO_3 under high temperature and hydroxyl reduction, (2) expansion of spaces between layers of carbon atoms owing to produced sodium interposition into carbon structures, and (3) reaction between active alkali intermediates and the carbon surface.[20,21] This also explains that the yield of A-BC (8.91%) was much lower than those of R-BC (62.05%) and BC800 (29.27%). The BET surface area analysis revealed that the NaOH activation of R-BC led to high enhancement of the surface area by a factor of 1193. The high surface area of A-BC (1991.59 m^2/g) was higher than those of various commercial activated carbons[4,22] (Table S2), while offering large active sites for adsorption of contaminants. Moreover, the scanning electron microscopy (SEM) images of A-BC (Figure S1) indicated that A-BC possessed the well-developed pore structure and various sizes of pores including micropores which could support the high surface area of A-BC.[22]

The proximate analysis results for all BCs listed in Table 1 showed significant changes in volatile and fixed carbons. Compared to R-BC, the contents of volatile carbon of BC800 and A-BC decreased from 73.14 to 18.04 and 19.58%, respectively, while the contents of fixed carbon increased from 23.22 to 67.92 and 70.96%, respectively. This was due to the thermal breakdown and release of volatile matter in carbohydrate fractions of BG feedstock during the heat treatment at high temperature resulting in the development of highly porous structures.[23] The ultimate analysis indicated that the C content in A-BC increased to 81.22% after the activation, while the O and H contents in A-BC markedly decreased to 7.42 and 0.84% compared to R-BC and BC800, respectively. The results were consistent with the previous studies which indicated the decomposition of O and H and the decrease in surface functional groups under high temperature and activated conditions.[4,24] The ratios of H/C, O/C, and (N

https://dx.doi.org/10.1021/acsomega.0c00983
ACS Omega 2020, 5, 13793−13801

+ O)/C significantly decreased after the activation, indicating that NaOH activation decreased the O-containing functional groups and polarity of BC while increasing the aromaticity and hydrophobicity of A-BC. This would come from decarboxylation and demethylation reactions and loss of volatile organic matters during the activation.[1,25] Additionally, A-BC showed higher hydrophobicity (low ratio of O/C) and aromaticity (low ratio of H/C) than various commercial activated carbons (Table S2), which could be beneficial for adsorption of hydrophobic contaminants onto the surface of A-BC because of hydrophobic interaction.

The X-ray diffraction (XRD) patterns listed in Figure S2 showed the wide peaks and the lack of sharp peaks, indicating the amorphous structures and a low degree of crystallinity in the BCs.[26,27] Moreover, the broad peaks at 23 and 43° in BC800 and A-BC revealed the formation of turbostratic crystallites which are mostly amorphous materials with a partly short-range order.[16,25−27]

The functional groups of all BCs were illustrated by Fourier-transform infrared spectroscopy (FTIR) spectra (Figure S3). In comparison with R-BC, the peaks of BC800 and A-BC at 2852 and 2922 cm^{-1} (aliphatic C−H stretching vibrations) completely disappeared, indicating the complete carbonization of the raw material via the heat treatment at high temperature and NaOH activation.[28] In contrast, the peak at 2122 cm^{-1} for C≡C stretching vibration showed strong intensity in BC800 and A-BC compared to R-BC.[29] Moreover, the peak intensity at 2122 cm^{-1} increased significantly after the activation, indicating that A-BC can provide more electron-donor sites, which are closely related to $\pi-\pi$ interactions between BCs and organic contaminants. The peak at 1575 cm^{-1}, corresponding to C=C stretching vibration, significantly increased in A-BC, revealing the high aromatization during the activation.[30] Compared to R-BC, the peak at about 1050−1060 cm^{-1} for C−O stretching vibration drastically decreased in BC800 and A-BC because of the loss of O-containing functional groups.[27] For A-BC, the peak at 1059 cm^{-1} (C−O) experienced a negative shift after the SMX adsorption, implying that the O-containing functional groups in A-BC interacted with the SMX. Both peaks at 1575 cm^{-1} (C=C) and 2120 cm^{-1} (C≡C) moved to 1591 and 2122 cm^{-1}, which would result from the interactions of these functional groups with SMX molecules during adsorption.

2.2. Effect of the Initial pH and Adsorption Mechanism. The initial pH can influence on the SMX adsorption onto BCs through altering properties of SMX and BCs. Owing to pK_1 = 1.6 and pK_2 = 5.7 (Table S3), the predominant species of SMX were SMX^+ at pH < 1.6, SMX^0 at 1.6 < pH < 5.7, and SMX^- at pH > 5.7.[1] The pH_{PZC} of R-BC, BC800, and A-BC were found to be 5.07, 4.19, and 5.63, respectively (Table 1 and Figure S4). The surface charges of BCs are positive with the solution pH less than their pH_{PZC}, otherwise they are negative.

As shown in Figure 1, compared with A-BC, R-BC and BC800 exhibited the low adsorption capacities for SMX at various pH values (less than 30 mg/g), which is possibly attributed to low surface areas of R-BC and BC800. For A-BC, the highest SMX adsorption was achieved at pH 3 (456 mg/g), but the increase in pH up to 10 resulted in a decrease in SMX adsorption as the similar trends were found from the previous studies.[13] Although the SMX adsorption capacity of A-BC varied with different pH values, the adsorption capacity (Q_e) did not change significantly between pH 1 and 9 (85.65% of maximal Q_e at pH 1; 78.60% of maximal Q_e at pH 9). Therefore, the SMX adsorption on A-BC was found to be applicable in a broad range of pH, which was favorable to practical applications of A-BC for wastewater and water treatment.

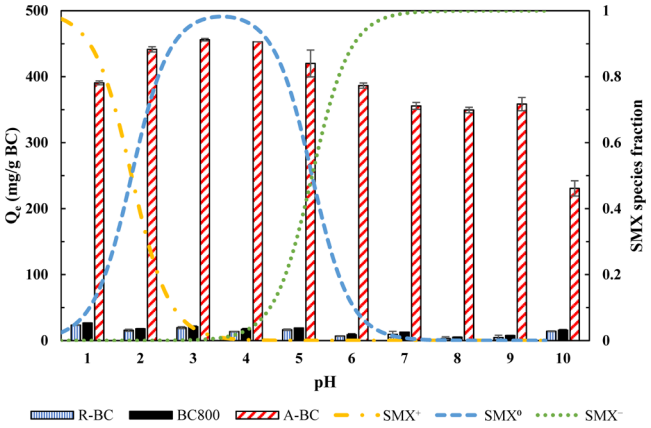

Figure 1. Adsorption of SMX onto all BCs. R-BC: raw biochar produced at 300 °C. BC800: biochar produced at 800 °C. A-BC: activated biochar.

The electrostatic interactions between the adsorbate and adsorbent surface significantly affected the adsorption of ionic compounds.[31] SMX^+ was predominant (79.92%) at pH 1 (Figure 1), and the surface charge of A-BC was near zero under acidic conditions (Figure S4). Therefore, the electrostatic interactions were not significant at pH 1. As seen in Figure 1, 85.65% of maximal Q_e was still observed at pH 1. In addition, $\pi-\pi$ electron donor−acceptor (EDA) interaction has been recognized as the major mechanism for sulfonamide adsorption on BCs.[11] SMX can serve as an electron acceptor because the sulfonamide group has the powerful electron-withdrawing capacity, and also, the heteroaromatic group becomes electron deficient because the high electronegativity of the O atom can reduce the electron density of the heteroaromatic group, while the graphitic surface of BC is electron rich and can serve as an electron donor.[11,32] Therefore, the noncovalent interaction ($\pi-\pi$ EDA) can form between the electron-rich π system (BC) and electron-deficient π system (SMX) via attractive interaction. Moreover, as shown in Tables S4 and S5, the contribution of SMX^+ to total adsorption was 91.86% at pH 1. The surface of A-BC includes C=C and C≡C groups (Figure S3), which can provide the electrons for $\pi-\pi$ EDA interaction. Thus, the adsorption at pH 1 may be governed by $\pi^+-\pi$ EDA interaction between the protonated aniline ring and the π-electron rich surface of A-BC.[11,31]

The maximum adsorption capacity of A-BC for SMX was achieved at pH 2−5. Because neutral SMX^0 molecules were predominant species and the surface of A-BC was positively charged at pH 2−5, the electrostatic interaction between A-BC and SMX was not responsible for the SMX adsorption onto A-BC. Therefore, other adsorption mechanisms such as $\pi-\pi$ EDA interaction, hydrophobic interaction, and hydrogen bond would involve in the adsorption of SMX onto A-BC. Although SMX has lowest solubility in water at pH 3.22, its solubility increases and decreases at pH values higher and lower than 3.22.[33] As shown in Figure 1, the adsorption capacities of A-BC for SMX decreased at pH values higher and lower than 3; therefore, the SMX adsorption on A-BC was negatively

https://dx.doi.org/10.1021/acsomega.0c00983
ACS Omega 2020, 5, 13793−13801

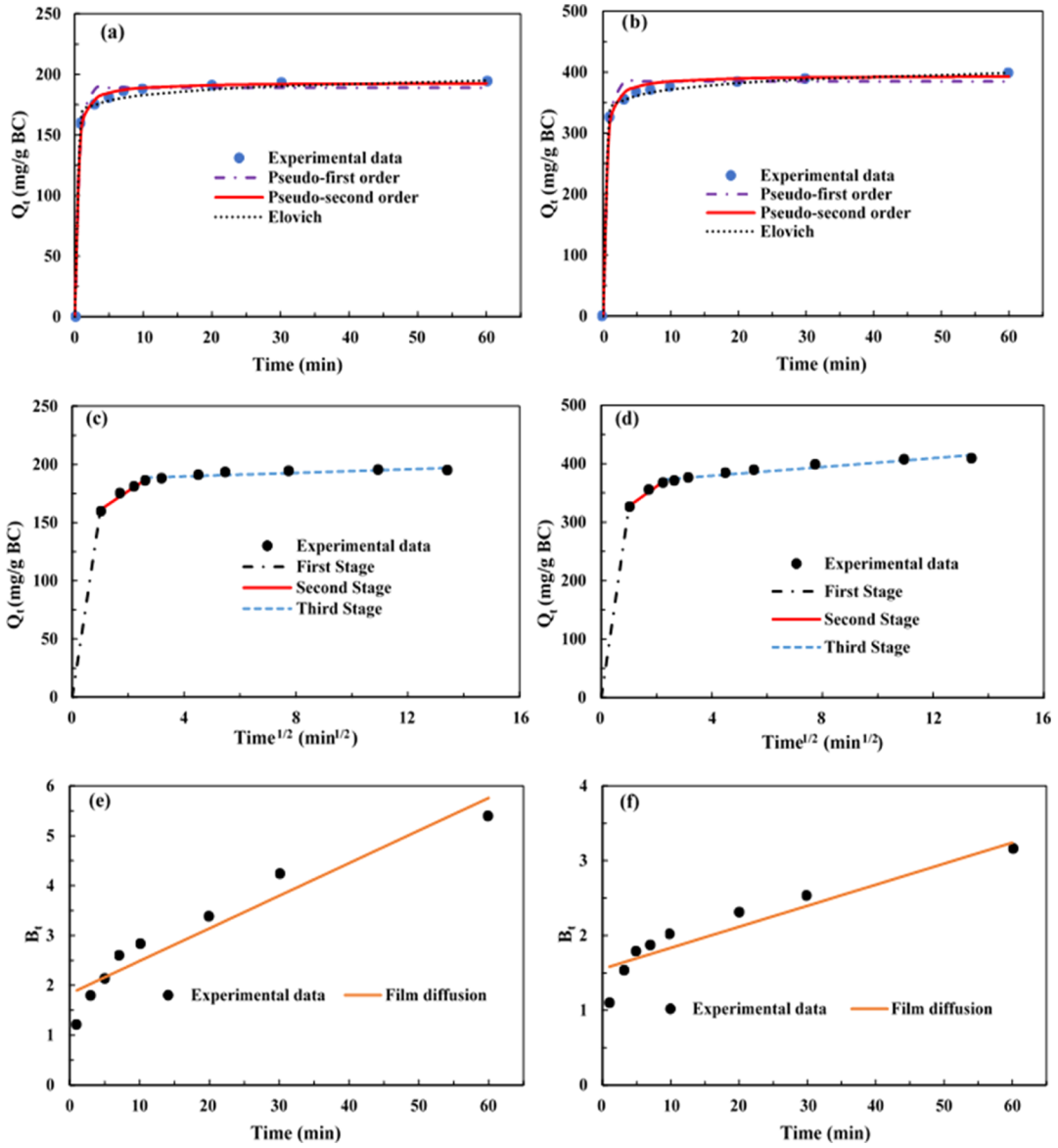

Figure 2. Adsorption kinetics of SMX onto A-BC by fitting the pseudo-first order, pseudo-second order, and Elovich (a,b) and intraparticle diffusion models (c,d) and the film diffusion model (e,f) under two different initial concentrations of 20 mg/L (a,c,e) and 100 mg/L (b,d,f).

influenced by increasing solubility of SMX. Thus, these findings also confirmed that hydrophobic interaction occurred between SMX and A-BC at pH 2−5, which was consistent with the previous studies.[1,9] Furthermore, strong hydrogen bonds could be generated between neutral sulfonamides and functional BCs, as reported by the previous studies.[29] From the analysis of FT-IR spectrum of A-BC before and after the SMX adsorption (Section 2.1), the O-containing functional groups of A-BC were found to involve in the SMX adsorption process. Hence, because of the high electronegativity of N and O atoms, hydrogen bond formation could occur between the O-containing functional groups of A-BC and the −NH− and $-NH_2$ groups in the SMX molecule.

In pH 6−10, SMX^- was predominant and the A-BC surface was negatively charged. Therefore, the K_d values gradually began to decline because of the existence of electrostatic repulsion (Table S4). Additionally, because of the deprotonation of SMX^- and the decrease in π electron acceptor capacity, $\pi-\pi$ EDA interaction significantly decreases at high pH.[3] However, at pH 6−10, some portion of SMX was still adsorbed onto the negatively charged A-BC. The previous study has reported that charge-assisted hydrogen bond (CAHB) interactions can occur between the negative BC surface and sulfonamides.[11] Moreover, as shown in Tables S4 and S5, the contribution of SMX^- to total adsorption was between 77.89 and 99.99% at pH 6−10. Therefore, the adsorption at this pH range may be attributed to negative CAHB between SMX^- and negatively charged A-BC. More specifically, SMX^- can first make H^+ exchange with the H_2O molecule and release the OH^- into aqueous solution, and OH^- can be neutralized by H^+ released from O-containing functional groups on the A-BC surface to form negative CAHB (eqs 2 and 3).[13,29]

$$SMX^- + H_2O \rightarrow SMX + OH^- \quad (2)$$

$$SMX + HO - BC = SMX^-\cdots H^+\cdots O^- - BC + H^+ \quad (3)$$

In conclusion, as shown in Figure S5, $\pi^+-\pi$ and $\pi-\pi$ EDA, hydrophobic, hydrogen bond, and CAHB interactions could be

https://dx.doi.org/10.1021/acsomega.0c00983
ACS Omega 2020, 5, 13793−13801

considered as possible adsorption mechanisms for adsorption of SMX onto A-BC.

2.3. Adsorption Kinetics. Kinetic studies are essential to comprehend the adsorption mechanisms and rate-limiting steps. In this study, the adsorption kinetics of SMX on A-BC was investigated under two initial concentrations of SMX (20 and 100 mg/L at pH 3). It is noteworthy that the data from two different concentrations exhibited the same trend. A fast adsorption occurred in a few minutes and reached the equilibrium after 60 min, which indicated a favorable interaction between SMX and A-BC (Figure 2).

The kinetic parameters determined from the adsorption results are listed in Table 2. With the high determination coefficient (R^2: 0.9933−0.9983), the PSO model (R^2: 0.9933−0.9983) was better fitted with experimental data than the PFO model (R^2: 0.9805−0.9886). In addition, the Q_e value calculated from the PSO model was closer to the experimental Q_e value, implying that chemisorption between SMX and A-BC was more important than physisorption.[1] The Elovich model was also well fitted to experimental data with high R^2 values (0.9933−0.9982) and low SSE (4.46−4.75).[1] The parameters (a and b) in the Elovich model for A-BC indicated a high value of the initial adsorption rate and low desorption (Table 2). Upon the assumptions for the Elovich model, strong chemical interactions would occur on the energetically heterogeneous surface of A-BC.[4] The adsorption process in porous materials is often controlled by intraparticle or film diffusion or both combined.[18] In this study, the intraparticle diffusion model was applied to the kinetic results for understanding possible rate-limiting steps. The key parameter (K_i) in the model indicated intraparticle diffusion limitation. The plots of Q_t against $t^{1/2}$ were distributed into three linear sections, representing three various stages (Figure 2c,d). The first stage was ascribed to the rapid diffusion of SMX into the external surface of A-BC. The second stage exhibited gradual adsorption and was attributed to intraparticle diffusion. In addition, the adsorption process reached the final equilibrium in the third stage, where the intraparticle diffusion rate decreased owing to the decrease in SMX concentration in the solution.[14,20] However, both second and third stages did not go through the origin, revealing that the intraparticle diffusion was not the sole rate-limiting step.[34]

Table 2. Summary of Kinetic Parameters of SMX Adsorption on A-BC

	20[a]	100[a]
Q_e[b]	194.99	409.03
Pseudo-First Order		
Q_e[c]	189.02	384.57
K_1	1.83	1.85
SSE	5.81	15.54
R^2	0.9886	0.9805
Pseudo-Second Order		
Q_e[c]	193.46	394.44
K_2	0.02	0.01
SSE	2.26	9.09
R^2	0.9983	0.9933
Elovich		
Q_e[c]	202.41	415.13
a	4.43×10^{11}	7.92×10^{10}
b	0.15	0.07
SSE	4.46	4.75
R^2	0.9933	0.9982
Intraparticle Diffusion		
K_{i1}	159.63	326.04
R^2	1	1
K_{i2}	16.00	33.93
R^2	0.9755	0.9834
K_{i3}	0.76	3.76
R^2	0.7282	0.9273
Film Diffusion (Boyd Equation)		
R^2	0.9129	0.9633

[a]Initial concentration of SMX (mg/L). [b]Observed value Q_e (mg/g). [c]Calculated value Q_e (mg/g).

To figure out the adsorption mechanism controlled by film diffusion, the kinetic data were further evaluated through the film diffusion model using the Boyd equation.[20] The calculated B_t values were plotted with time t, as displayed in Figure 2e,f. When the data points were linear and across the origin, intraparticle diffusion controlled the transfer of adsorbate molecules.[35] As shown in Figure 2e,f, the linear lines from two different initial concentrations of SMX did not go through the origin, revealing that film diffusion also participated in the entire adsorption process.[35] Therefore, both film diffusion and intraparticle diffusion may play a significant part during the process of SMX adsorption onto A-BC.

2.4. Adsorption Isotherm. For comprehensively understanding the nature of interactions between SMX and A-BC, the isotherm models (Langmuir, Freundlich, Temkin, and Dubinin-Redushckevich) were fitted to the experimental results (Table 3 and Figure S6). As summarized in Table 3, compared to the Freundlich model (R^2 = 0.9145), the isotherm results were better matched with the Langmuir model (R^2 = 0.9418), indicating that monolayer adsorption of SMX molecules would occur on the homogeneous surface of A-BC.[36] Moreover, the low value of R_L (separation constant; the adsorption is irreversible at $R_L = 0$, favorable at $0 < R_L < 1$, linear at $R_L = 1$, and unfavorable at $R_L > 1$) was calculated from

Table 3. Summary of Isotherm Model Parameters for SMX Adsorption on A-BC

Langmuir Model	
Q_m	424.66
K_L	6.12
R_L	0.016
SSE	28.63
R^2	0.9418
Freundlich Model	
K_f	286.05
N	7.55
SSE	34.71
R^2	0.9145
Dubinin-Radushkevich Model	
K_{DR}	429.72
B_D	0.00006
E	91.29
SSE	37.37
R^2	0.9009
Temkin Model	
K_T	915.18
b_T	55.69
SSE	19.27
R^2	0.9736

https://dx.doi.org/10.1021/acsomega.0c00983
ACS Omega 2020, 5, 13793−13801

Table 4. Thermodynamic Parameters for the Adsorption of SMX on A-BC

			ΔG (kJ/mol)		
concentration (mg/L)	ΔH (kJ/mol)	ΔS (J/mol·K)	T = 293 K	T = 303 K	T = 313 K
100	2.120	23.372	−4.732	−4.965	−5.199
50	6.184	49.682	−8.380	−8.877	−9.374

the Langmuir model, which suggested that the SMX adsorption onto A-BC was favorable in the SMX concentration used for this study (Table 3).[36] The value of the heterogeneity factor $1/n$ (0.13) from the Freundlich model, close to zero, indicated that A-BC presented a high heterogeneity degree.[20] Moreover, the Temkin model exhibited the highest R^2 (0.9736) and lowest SSE (19.27) among all of the models. Based on the assumption of the Temkin model that adsorption heat is reduced linearly with the surface coverage of the adsorbent, the chemisorptive interaction was dominant in the adsorption process.[37] Furthermore, the obtained mean free energy value (E) from the Dubinin-Radushkevich model (91.29 kJ/mol) was bigger than 8 kJ/mol, indicating that strong chemisorption happened on the surface of A-BC, which supported the result of kinetics analysis.[37]

The A-BC exhibited a maximum adsorption capacity of 424.66 mg/g, which was higher than those of different adsorbents (Table S1). The previous studies have reported that the SMX adsorption capacity showed positive correlation with surface areas of different adsorbents.[1] Thus, in this study, the high Q_e value of A-BC may be ascribed to its high surface area (1991.59 m^2/g) after NaOH activation. Moreover, for figuring out potential of A-BC for commercial application, three commercial ACs (Calgon F400, Darco G-60, and Norit GAC) were also used for SMX adsorption. Surprisingly, the Q_e value of A-BC was higher than those of Calgon F400 (312.14 mg/g), Darco G-60 (328.83 mg/g), and Norit GAC (377.5 mg/g), which demonstrated the great potential of A-BC for the treatment of SMX in wastewater.

2.5. Thermodynamic Study. The thermodynamic parameters were determined based on the impact of temperature (293−313 K) on SMX adsorption onto A-BC. The ΔG^0 values were negative under all investigated temperatures and initial concentrations, implying the spontaneous adsorption of SMX onto A-BC (Table 4).[36] In addition, the ΔG^0 value decreased with the increase in temperature, revealing that the affinity of SMX onto A-BC also increased at higher temperature. Furthermore, the absolute values of ΔG^0 obtained at an initial concentration of 50 mg/L were higher than those of 100 mg/L, indicating that SMX adsorption might be more spontaneous at lower initial concentration. This would be explained by the fact that higher initial SMX concentration could cause higher competition of SMX molecules for the available active sites on the surface of A-BC. The positive values of ΔH^0 (2.120−6.184 kJ/mol) evidenced that the adsorption process was endothermic and inclined to chemisorption as physisorption often shows exothermic reactions.[36] Meanwhile, the values of ΔS^0 (23.372−49.682 J/mol·K) were positive, suggesting that the randomness was enhanced at the contact area of solid−liquid and the adsorption was spontaneous in nature.[38]

2.6. Applications of A-BC for Treatment of Other Emerging Contaminants and Wastewater. While the A-BC was used for adsorption of SMX in this study, the adsorption capacities of A-BC for tetracycline and bisphenol A in water were also evaluated. The adsorption capacity of A-BC for tetracycline under the selected condition (0.01 g of BC, 100 mL of 100 mg/L tetracycline, initial pH 6, and 3 d) was 307 mg/g, which was higher than those of commercial activated carbons and activated BCs (96−290 mg TC/g BC) and other BCs reported in the previous study.[4] The adsorption capacity of A-BC for bisphenol A under the selected condition (0.01 g of BC, 100 mL of 70 mg/L bisphenol A, initial pH of 6, and 3 d) was also estimated to be 356 mg of bisphenol A/g BC, which was greater than those of commercial activated carbons (130−263 bisphenol A mg/g) and other BCs reported in the previous study.[12]

In order to see practical feasibility of A-BC for treatment of antibiotics (SMX) in real wastewater containing multiple pollutants, SMX was added to the wastewater taken from the second lagoon at the dairy farm of Southwest Dairy Center, Tarleton State University (Stephenville, TX). Please see multiple pollutants in the dairy wastewater, which are listed in Table S6. Under the same adsorption conditions, compared to SMX adsorption onto A-BC in DI water, the adsorption capacity of A-BC for SMX in the dairy wastewater was reduced by 38.47% (Figure S7). This result clearly supports the fact that the presence of various organic and inorganic contaminants in the wastewater (Table S6) could compete with SMX for the active adsorption sites of A-BC, although understanding of effects of the individual pollutant is extremely challenging.

2.7. Regeneration Study. The regeneration of adsorbents is of great importance for development of cost-effective processes. Thus, it is important for A-BC to be effectively regenerated for long term reuse for removal of SMX in water. In this study, NaOH-driven desorption was selected as one of the possible desorption methods, although the previous studies also reported other desorption agents for regeneration of contaminant-saturated carbon adsorbents such as KOH, methanol, and ethanol.[39,40] Various concentrations of NaOH solution were used to regenerate A-BC after A-BC was fully saturated with SMX. As presented in Figure S8, the readsorption capacity was the highest (397.65 mg/g) after regeneration using 0.2 M NaOH, and the NaOH concentration was higher than 0.2 M and resulted in the decrease in readsorption capacity. Previous studies also reported that the high regeneration capacity of BCs was observed using 0.1 M NaOH as the dilute NaOH could result in the formation of more interconnected pore structures.[18,41] However, the carbon structure might be damaged or deformed under high concentration of NaOH, leading to the lower readsorption capacity. In addition, four cycles of adsorption−desorption were also conducted using 0.2 M NaOH in the present study. As shown in Figure 3, the regeneration efficiency remained at 91.19 and 64.60% after the first and fourth cycles, indicating high potential of NaOH-driven regeneration of A-BC under optimization of regeneration conditions.

Therefore, owing to its inexpensive feedstock, high adsorption, regeneration capacities, and possible adsorption of various contaminants, A-BC can be one of the highly effective adsorbents for treatment of various organic contaminants in water and wastewater.

https://dx.doi.org/10.1021/acsomega.0c00983
ACS Omega 2020, 5, 13793−13801

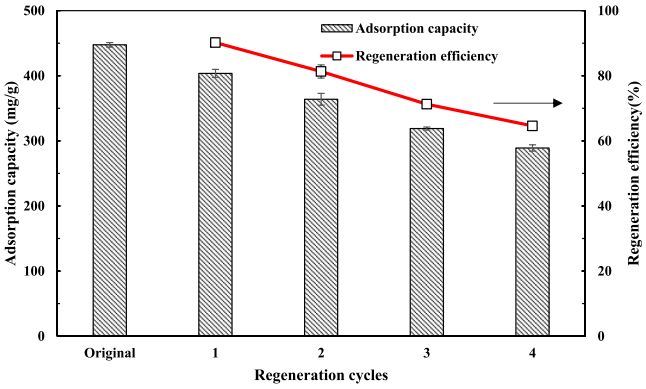

Figure 3. Reusability test of A-BC using 0.2 M NaOH.

3. CONCLUSIONS

The NaOH-activated BC made from forage BG showed a high surface area (1991.59 m^2/g) and adsorption capacity for SMX (425 mg/g BC), which was higher than various adsorbents including commercial ACs. The experimental results were well fitted by PSO and Elovich kinetic and Temkin isotherm models, revealing the strong chemisorptive interaction between SMX and A-BC. Moreover, both intraparticle diffusion and film diffusion affected the rate-limiting steps in the adsorption process. Additionally, the thermodynamic parameters implied the spontaneity and endothermic characteristic of SMX adsorption on A-BC. Furthermore, the regeneration of A-BC via NaOH-driven desorption revealed the great potential for practical application of A-BC.

4. MATERIALS AND METHODS

4.1. Materials. All chemicals used for this study were bought from Sigma-Aldrich (St. Louis, Missouri, U.S.). BG was obtained from a local hay shop (Stephenville, TX, U.S.). Three commercial activated carbons (Darco G-60, Norit GAC, and Calgon F400) were acquired from Sigma-Aldrich and Calgon Carbon.

4.2. Production of BCs. BG, dried and sieved (<500 μm), was utilized as the feedstock for BC. BG (10 g) was introduced into the quartz-tube furnace (MTI Corporation, Richmond, U.S.) and converted to BC under 300 °C for 15 min with 2 L/min of N_2 flow. The first resulting raw BC was named "R-BC". The pyrolysis and activation conditions in the current study were the same as those in the previous studies, which showed the great performance for preparing the activated BCs.[4,42] NaOH solution (40 mL, 4 M) and 3 g of R-BC were mixed together at 20 °C for 2 h and then dried at 105 °C overnight. Afterward, the dry mixture was pyrolyzed under the activation conditions (800 °C, 8 °C/min, 2 L/min of N_2, and 2 h reaction). The activated BC was named "A-BC". As a control, the BG was directly carbonized at 800 °C for 2 h with 8 °C/min, which was named "BC800". The R-BC, A-BC, and BC800 were washed with 3 M HCl (50 mL 3 M HCl/g BC) for 1 d and then repeated to be flushed with deionized water until the pH of filtered water became neutral. All BCs were dried at 105 °C and sieved (<106 μm) for following tests. The yields of BCs were evaluated using eq 4

$$\text{yield}\ (\%) = \frac{A}{B} \times 100 \tag{4}$$

where B represents the weight of BG and A represents the weight of BCs after washing and drying.

4.3. Physicochemical Properties of BCs. Chemical compositions of all BCs were determined using an elemental analyzer (Robert Microlit Lab, NJ, USA), and a proximate analysis was carried out based on ASTM standard D7582-10.[43] The BET surface area was analyzed through the measurements of N_2 sorption at 77 K (Particle Technology Lab, Downers Grove, USA). Functional groups in all BCs were evaluated using an FT-IR spectrometer (Bruker Optik GmbH, Ettlingen, Germany). An X-ray diffractometer (MiniFlex II, DE, USA), operated at 30 kV and 15 mA, was used to evaluate the crystalline structures on the surface of BCs. The surface morphologies of BCs were examined using a scanning electron microscope (S-4800, Hitachi Co., Japan). The pH of zero point charges (pH_{PZC}) of BCs was evaluated through the procedures described in the previous work.[4] Please see the detailed characterization methods in the Supporting Information.

4.4. Batch Adsorption Experiment. The adsorption of SMX on all BCs (R-BC, BC800, and A-BC) was performed at pH 1−10 under the selected conditions. The batch adsorption tests were initiated by mixing 0.01 g of BC with 100 mL of 100 mg/L SMX solution in 250 mL Erlenmeyer flasks for 3 d at 20 °C. The kinetic, isotherm, thermodynamic, and regeneration studies were conducted at the selected optimal pH obtained from the abovementioned experiments.

The adsorption kinetics were studied by mixing 0.01 g of BC with 100 mL of SMX solution (20 and 100 mg/L). The adsorption isotherm experiments were carried out with 100 mL of SMX solution (10−100 mg/L) and 0.01 g of BC for 3 d.

For the thermodynamic analysis, SMX adsorption onto A-BC was conducted by mixing 100 mL of SMX solution (50 and 100 mg/L) and 0.01 g of BC at 20−40 °C for 3 d.

To see the possible practical application of A-BC for treatment of real wastewater, the adsorption experiment was conducted by stirring 0.01 g of A-BC and 100 mL of wastewater sampled from the second lagoon at the dairy farm at Southwest Dairy Center, Tarleton State University (Stephenville, TX) for 3 d. The dairy wastewater from the second lagoon at the dairy farm contained various organic and inorganic compounds spiked with 100 mg/L SMX at pH 6.

4.5. Regeneration Study. To regenerate and reuse the SMX-saturated A-BC, NaOH was selected as the desorption agent in this study. After 3 d of adsorption, the SMX saturated A-BC was separated from SMX solution and added into the same volume of NaOH solution (0.1−2.0 M NaOH) for the NaOH-driven desorption for 1 d. After NaOH desorption, the A-BC was separated from NaOH solution and dried at 65 °C. The conditions for readsorption experiments were the same as those described in Section 4.4. Four cycles of adsorption−desorption were performed using 0.2 M NaOH solution. The regeneration efficiency of A-BC was calculated using eq 5

$$\text{regeneration efficiency}\ (\%) = \frac{Q_n}{Q_0} \times 100 \tag{5}$$

where Q_0 is the initial Q_e and Q_n is the Q_e at n generation cycles.

4.6. Modeling of Adsorption Kinetics, Isotherms, and Thermodynamics. In this study, the results obtained from the batch adsorption experiments in Section 4.4 were fitted to five kinetic models for adsorption kinetics and four isotherm models for the adsorption isotherm while used for determining thermodynamic parameters including standard enthalpy

https://dx.doi.org/10.1021/acsomega.0c00983
ACS Omega 2020, 5, 13793−13801

change (ΔH^0), standard entropy change (ΔS^0), and standard Gibbs free energy change (ΔG^0).[38] The detailed descriptions for the models and the thermodynamic properties are listed in Table S7.

4.7. Chemical and Data Analysis. The aqueous SMX concentration was evaluated through the high-performance liquid chromatography (LC-2030C model, SHIMADZU, Torrance, CA, U.S.) with a C18 column (3.6 μm XB-C18). The operation conditions included the mobile phase [methanol/water (33:67, volume ratio) with 0.1% formic acid], a flow rate of 0.6 mL/min, and a UV detector at 265 nm.

Adsorption capacities at equilibrium and time t, Q_e (mg/g) and Q_t (mg/g), were determined using eqs 6 and 7

$$Q_e = \frac{(C_i - C_e) \times V}{M} \quad (6)$$

$$Q_t = \frac{(C_i - C_t) \times V}{M} \quad (7)$$

where C_i, C_e, and C_t represent the SMX concentration of the initial, equilibrium time, and time t (mg/L), respectively, V represents the solution volume (L), and M represents the mass of BC used in adsorption tests (g).

The following empirical equation was utilized to calculate the quantitative contribution of single SMX species to overall sorption in a given pH value

$$K_d = K_d^- \alpha^- + K_d^0 \alpha^0 + K_d^+ \alpha^+ \quad (8)$$

where α^-, α^0, and α^+ represent the mass fraction of SMX^-, SMX^0, and SMX^+, respectively, K_d, K_d^-, K_d^0, and K_d^+ (L/kg) represent the adsorption coefficient of total, α^-, α^0, and α^+, respectively. The contribution percentage of various SMX species was determined by $K_d^- \alpha^- / K_d$ for SMX^-, $K_d^0 \alpha^0 / K_d$ for SMX^0, and $K_d^+ \alpha^+ / K_d$ for SMX^+.

■ ASSOCIATED CONTENT

Supporting Information

The Supporting Information is available free of charge at https://pubs.acs.org/doi/10.1021/acsomega.0c00983.

Methods for characterization of BCs; maximum adsorption capacity (Q_m) of various adsorbents for SMX; characteristics of various activated carbons; physicochemical characteristics of SMX; sorption coefficients for three SMX species on A-BC; contribution of different SMX species to the overall sorption on A-BC; characteristics of lagoon wastewater from dairy farm; adsorption isotherm, kinetic, and thermodynamic models; SEM; XRD; FT-IR; pH_{PZC}; mechanisms for SMX adsorption on A-BC; adsorption isotherm of SMX on A-BC; effect of different NaOH concentrations on the regeneration of A-BC; and adsorption of SMX onto A-BC in DI water and real wastewater (PDF)

■ AUTHOR INFORMATION

Corresponding Author

Eunsung Kan − *Department of Biological and Agricultural Engineering & Texas A&M AgriLife Research Center, Texas A&M University, College Station, Texas 76401, United States; Department of Wildlife, Sustainability, and Ecosystem Sciences, Tarleton State University, Stephenville, Texas 76401, United States;* orcid.org/0000-0001-6298-6096; Phone: +1-254-968-4144; Email: Eunsung.Kan@ag.tamu.edu; Fax: +1-254-968-3759

Author

Shengquan Zeng − *Department of Biological and Agricultural Engineering & Texas A&M AgriLife Research Center, Texas A&M University, College Station, Texas 76401, United States*

Complete contact information is available at: https://pubs.acs.org/10.1021/acsomega.0c00983

Author Contributions

S.Z. conducted all of the experiments and wrote the original manuscript. E.K. provided the concept and experimental design for this research work and revised the manuscript.

Notes

The authors declare no competing financial interest.

■ ACKNOWLEDGMENTS

This work was supported by Texas A&M University Chancellor Research Initiative Fund.

■ REFERENCES

(1) Jang, H. M.; Yoo, S.; Park, S.; Kan, E. Engineered biochar from pine wood: Characterization and potential application for removal of sulfamethoxazole in water. *Environ. Eng. Res.* **2018**, *24*, 608−617.

(2) Yao, Y.; Gao, B.; Chen, H.; Jiang, L.; Inyang, M.; Zimmerman, A. R.; Cao, X.; Yang, L.; Xue, Y.; Li, H. Adsorption of sulfamethoxazole on biochar and its impact on reclaimed water irrigation. *J. Hazard. Mater.* **2012**, *209−210*, 408−413.

(3) Yao, Y.; Zhang, Y.; Gao, B.; Chen, R.; Wu, F. Removal of sulfamethoxazole (SMX) and sulfapyridine (SPY) from aqueous solutions by biochars derived from anaerobically digested bagasse. *Environ. Sci. Pollut. Res.* **2018**, *25*, 25659−25667.

(4) Jang, H. M.; Yoo, S.; Choi, Y.-K.; Park, S.; Kan, E. Adsorption isotherm, kinetic modeling and mechanism of tetracycline on Pinus taeda-derived activated biochar. *Bioresour. Technol.* **2018**, *259*, 24−31.

(5) Zhao, H.; Liu, X.; Cao, Z.; Zhan, Y.; Shi, X.; Yang, Y.; Zhou, J.; Xu, J. Adsorption behavior and mechanism of chloramphenicols, sulfonamides, and non-antibiotic pharmaceuticals on multi-walled carbon nanotubes. *J. Hazard. Mater.* **2016**, *310*, 235−245.

(6) Chen, H.; Gao, B.; Li, H. Removal of sulfamethoxazole and ciprofloxacin from aqueous solutions by graphene oxide. *J. Hazard. Mater.* **2015**, *282*, 201−207.

(7) Calisto, V.; Ferreira, C. I. A.; Oliveira, J. A. B. P.; Otero, M.; Esteves, V. I. Adsorptive removal of pharmaceuticals from water by commercial and waste-based carbons. *J. Environ. Manage.* **2015**, *152*, 83−90.

(8) Gao, J.; Pedersen, J. A. Adsorption of sulfonamide antimicrobial agents to clay minerals. *Environ. Sci. Technol.* **2005**, *39*, 9509−9516.

(9) Reguyal, F.; Sarmah, A. K.; Gao, W. Synthesis of magnetic biochar from pine sawdust via oxidative hydrolysis of FeCl2 for the removal sulfamethoxazole from aqueous solution. *J. Hazard. Mater.* **2017**, *321*, 868−878.

(10) Braghiroli, F. L.; Bouafif, H.; Neculita, C. M.; Koubaa, A. Activated Biochar as an Effective Sorbent for Organic and Inorganic Contaminants in Water. *Water, Air, Soil Pollut.* **2018**, *229*, 230.

(11) Peiris, C.; Gunatilake, S. R.; Mlsna, T. E.; Mohan, D.; Vithanage, M. Biochar based removal of antibiotic sulfonamides and tetracyclines in aquatic environments: A critical review. *Bioresour. Technol.* **2017**, *246*, 150−159.

(12) Choi, Y.-K.; Kan, E. Effects of pyrolysis temperature on the physicochemical properties of alfalfa-derived biochar for the adsorption of bisphenol A and sulfamethoxazole in water. *Chemosphere* **2019**, *218*, 741−748.

(13) Ahmed, M. B.; Zhou, J. L.; Ngo, H. H.; Guo, W.; Johir, M. A. H.; Sornalingam, K. Single and competitive sorption properties and

mechanism of functionalized biochar for removing sulfonamide antibiotics from water. *Chem. Eng. J.* **2017**, *311*, 348−358.
(14) Yang, X.; Xu, G.; Yu, H.; Zhang, Z. Preparation of ferric-activated sludge-based adsorbent from biological sludge for tetracycline removal. *Bioresour. Technol.* **2016**, *211*, 566−573.
(15) Rajapaksha, A. U.; Vithanage, M.; Ahmad, M.; Seo, D.-C.; Cho, J.-S.; Lee, S.-E.; Lee, S. S.; Ok, Y. S. Enhanced sulfamethazine removal by steam-activated invasive plant-derived biochar. *J. Hazard. Mater.* **2015**, *290*, 43−50.
(16) Taheran, M.; Naghdi, M.; Brar, S. K.; Knystautas, E. J.; Verma, M.; Ramirez, A. A.; Surampalli, R. Y.; Valero, J. R. Adsorption study of environmentally relevant concentrations of chlortetracycline on pinewood biochar. *Sci. Total Environ.* **2016**, *571*, 772−777.
(17) Wang, Z.; Keshwani, D. R.; Redding, A. P.; Cheng, J. J. Sodium hydroxide pretreatment and enzymatic hydrolysis of coastal Bermuda grass. *Bioresour. Technol.* **2010**, *101*, 3583−3585.
(18) Jang, H. M.; Kan, E. A novel hay-derived biochar for removal of tetracyclines in water. *Bioresour. Technol.* **2019**, *274*, 162−172.
(19) Tu, B.; Wen, R.; Wang, K.; Cheng, Y.; Deng, Y.; Cao, W.; Zhang, K.; Tao, H. Efficient removal of aqueous hexavalent chromium by activated carbon derived from Bermuda grass. *J. Colloid Interface Sci.* **2020**, *560*, 649−658.
(20) Martins, A. C.; Pezoti, O.; Cazetta, A. L.; Bedin, K. C.; Yamazaki, D. A. S.; Bandoch, G. F. G.; Asefa, T.; Visentainer, J. V.; Almeida, V. C. Removal of tetracycline by NaOH-activated carbon produced from macadamia nut shells: Kinetic and equilibrium studies. *Chem. Eng. J.* **2015**, *260*, 291−299.
(21) Foo, K. Y.; Hameed, B. H. Potential of jackfruit peel as precursor for activated carbon prepared by microwave induced NaOH activation. *Bioresour. Technol.* **2012**, *112*, 143−150.
(22) Yan, L.; Liu, Y.; Zhang, Y.; Liu, S.; Wang, C.; Chen, W.; Liu, C.; Chen, Z.; Zhang, Y. $ZnCl_2$ modified biochar derived from aerobic granular sludge for developed microporosity and enhanced adsorption to tetracycline. *Bioresour. Technol.* **2020**, *297*, 122381.
(23) Park, J.; Hung, I.; Gan, Z.; Rojas, O. J.; Lim, K. H.; Park, S. Activated carbon from biochar: influence of its physicochemical properties on the sorption characteristics of phenanthrene. *Bioresour. Technol.* **2013**, *149*, 383−389.
(24) Wang, H.; Chu, Y.; Fang, C.; Huang, F.; Song, Y.; Xue, X. Sorption of tetracycline on biochar derived from rice straw under different temperatures. *PLoS One* **2017**, *12*, No. e0182776.
(25) Luo, J.; Li, X.; Ge, C.; Müller, K.; Yu, H.; Huang, P.; Li, J.; Tsang, D. C. W.; Bolan, N. S.; Rinklebe, J.; Wang, H. Sorption of norfloxacin, sulfamerazine and oxytetracycline by KOH-modified biochar under single and ternary systems. *Bioresour. Technol.* **2018**, *263*, 385−392.
(26) Mondal, S.; Aikat, K.; Halder, G. Ranitidine hydrochloride sorption onto superheated steam activated biochar derived from mung bean husk in fixed bed column. *J. Environ. Chem. Eng.* **2016**, *4*, 488−497.
(27) Zhu, X.; Liu, Y.; Qian, F.; Zhou, C.; Zhang, S.; Chen, J. Preparation of magnetic porous carbon from waste hydrochar by simultaneous activation and magnetization for tetracycline removal. *Bioresour. Technol.* **2014**, *154*, 209−214.
(28) Yakout, S. M. Monitoring the Changes of Chemical Properties of Rice Straw−Derived Biochars Modified by Different Oxidizing Agents and Their Adsorptive Performance for Organics. *Biorem. J.* **2015**, *19*, 171−182.
(29) Ahmed, M. B.; Zhou, J. L.; Ngo, H. H.; Guo, W.; Johir, M. A. H.; Belhaj, D. Competitive sorption affinity of sulfonamides and chloramphenicol antibiotics toward functionalized biochar for water and wastewater treatment. *Bioresour. Technol.* **2017**, *238*, 306−312.
(30) Ahmed, M. B.; Zhou, J. L.; Ngo, H. H.; Guo, W.; Johir, M. A. H.; Sornalingam, K.; Sahedur Rahman, M. Chloramphenicol interaction with functionalized biochar in water: sorptive mechanism, molecular imprinting effect and repeatable application. *Sci. Total Environ.* **2017**, *609*, 885−895.
(31) Zheng, H.; Wang, Z.; Zhao, J.; Herbert, S.; Xing, B. Sorption of antibiotic sulfamethoxazole varies with biochars produced at different temperatures. *Environ. Pollut.* **2013**, *181*, 60−67.
(32) Tan, X.; Liu, Y.; Zeng, G.; Wang, X.; Hu, X.; Gu, Y.; Yang, Z. Application of biochar for the removal of pollutants from aqueous solutions. *Chemosphere* **2015**, *125*, 70−85.
(33) Dahlan, R.; Mcdonald, C.; Sunderland, V. B. Solubilities and intrinsic dissolution rates of sulphamethoxazole and trimethoprim. *J. Pharm. Pharmacol.* **1987**, *39*, 246−251.
(34) He, J.; Dai, J.; Zhang, T.; Sun, J.; Xie, A.; Tian, S.; Yan, Y.; Huo, P. Preparation of highly porous carbon from sustainable α-cellulose for superior removal performance of tetracycline and sulfamethazine from water. *RSC Adv.* **2016**, *6*, 28023−28033.
(35) Zhang, L.; Song, X.; Liu, X.; Yang, L.; Pan, F.; Lv, J. Studies on the removal of tetracycline by multi-walled carbon nanotubes. *Chem. Eng. J.* **2011**, *178*, 26−33.
(36) Pezoti, O.; Cazetta, A. L.; Bedin, K. C.; Souza, L. S.; Martins, A. C.; Silva, T. L.; Santos Júnior, O. O.; Visentainer, J. V.; Almeida, V. C. NaOH-activated carbon of high surface area produced from guava seeds as a high-efficiency adsorbent for amoxicillin removal: Kinetic, isotherm and thermodynamic studies. *Chem. Eng. J.* **2016**, *288*, 778−788.
(37) Tang, L.; Yu, J.; Pang, Y.; Zeng, G.; Deng, Y.; Wang, J.; Ren, X.; Ye, S.; Peng, B.; Feng, H. Sustainable efficient adsorbent: Alkali-acid modified magnetic biochar derived from sewage sludge for aqueous organic contaminant removal. *Chem. Eng. J.* **2018**, *336*, 160−169.
(38) Shin, H. S.; Kim, J.-H. Isotherm, kinetic and thermodynamic characteristics of adsorption of paclitaxel onto Diaion HP-20. *Process Biochem.* **2016**, *51*, 917−924.
(39) Han, Y.; Cao, X.; Ouyang, X.; Sohi, S. P.; Chen, J. Adsorption kinetics of magnetic biochar derived from peanut hull on removal of Cr (VI) from aqueous solution: effects of production conditions and particle size. *Chemosphere* **2016**, *145*, 336−341.
(40) Reguyal, F.; Sarmah, A. K.; Gao, W. Synthesis of magnetic biochar from pine sawdust via oxidative hydrolysis of $FeCl_2$ for the removal sulfamethoxazole from aqueous solution. *J. Hazard. Mater.* **2017**, *321*, 868−878.
(41) Zhou, Y.; Liu, X.; Xiang, Y.; Wang, P.; Zhang, J.; Zhang, F.; Wei, J.; Luo, L.; Lei, M.; Tang, L. Modification of biochar derived from sawdust and its application in removal of tetracycline and copper from aqueous solution: Adsorption mechanism and modelling. *Bioresour. Technol.* **2017**, *245*, 266−273.
(42) Jang, H. M.; Kan, E. Engineered biochar from agricultural waste for removal of tetracycline in water. *Bioresour. Technol.* **2019**, *284*, 437−447.
(43) ASTM, A., D7582−10. Standard Test Methods for Proximate Analysis of Coal and Coke by Macro Thermogravimetric Analysis. *Annual Book of ASTM Standards*; American Society for Testing and Materials: West Conshohocken, PA, 2010.

https://dx.doi.org/10.1021/acsomega.0c00983
ACS Omega 2020, 5, 13793−13801